Universidad Carlos III de Madrid
e-Archivo

Institutional Repository

This document is published in:

Lenticular arrays based on liquid crystals

V. Urruchi del Pozo[*1], J.F. Algorri Genaro[1], J.M. Sánchez-Pena[1], M.A. Geday[2], X.Q. Arregui[2], and N. Bennis[2]

[1]Grupo de Displays & Aplicaciones Fotónicas, Dept. de Tecnologia Electrónica, E.P.S.,
Universidad Carlos III, Butarque 15, 28911 Leganés, Madrid, Spain
[2]Grupo de Cristales Liquidos, Dept. de Tecnologia Fotónica, E.T.S.I. Telecomunicación,
Ciudad Universitaria s/n, 28040 Madrid, Spain

Abstract: Lenticular array products have experienced a growing interest in the last decade due to the very wide range of applications they can cover. Indeed, this kind of lenses can create different effects on a viewing image such as 3D, flips, zoom, etc. In this sense, lenticular based on liquid crystals (LC) technology is being developed with the aim of tuning the lens profiles simply by controlling the birefringence electrically. In this work, a LC lenticular lens array has been proposed to mimic a GRIN lentic− ular lens array but adding the capability of tuning their lens profiles. Comb control electrodes have been designed as pattern masks for the ITO on the upper substrate. Suitable high resistivity layers have been chosen to be deposited on the control electrode generating an electric field gradient between teeth of the same electrode. Test measurements have allowed us to demonstrate that values of phase retardations and focal lengths, for an optimal driving waveform, are fairly in agreement. In addition, results of focusing power of tuneable lenses were compared to those of conventional lenses. The behaviour of both kinds of lenses has revealed to be mutually similar for focusing collimated light and for refracting images.

Keywords: Liquid crystal lenticular array, GRIN lens, high resistivity layer, birefringence electrically controlled.

1. Introduction

Liquid crystals (LC) are a competitive technology being adopted by many research works since the last fifty years. Distinctive properties of these materials, derived from the tuning capacity of their anisotropic properties, are unique for some applications.

On one hand, research on non-photonic applications of liquid crystals is opened and very new approaches are being developed. One example are microwaves devices, a recent and very active research field focused on building antennas, phase shifters or filters based on liquid crystals [1]. However, on the other hand, photonic applications based on these materials have already been extensively researched; covering many diverse fields. Nanotechnology works are dealing with carbon nanotubes applications and liquid crystal – nanoparticles interactions [2], security is treating cryptographic applications [3] and optical communications are handling optical components that are easily integrated in optical fibre systems. Some examples are modulators or filters [4], distributed sensors [5], beam steering devices [6], aberration correction spatial light modulators [7], bio-optics applications [8] and optical lenses [9].

Particularly, LC lenses with electrically controllable focal length have been reported to show many feasible approaches since the first patent of the invention in 1980 [10]. This essential focusing property represents a significant improvement compared to conventional fixed lenses because the use of mechanical moving parts may be avoided. Also, static lenses involve complex manufacturing processes for creating the surface curvature, procedures that get more complicated if size of devices is reduced to micrometric order. Instead, plane surfaces of LC devices make the assembly to standard optics easier, for example, attaching to an optical fibre and can diminish production costs. LC lenses share their applications with conventional fixed lenses. In addition to the advantages of LC lenses previously mentioned, lenses arrays based on this technology have shown another advantages according to the specific application. Small size and light weight are some strict constraints, for example, in military applications. Many research works have been reported such as focusing a light beam on a spot, beam steering control in curved trajectories of light in bar--code scanners or imaging in optical systems using Fresnel lenses. Low driving voltages, low power consumption and trans-missive/reflective operation modes are also benefits for driving the devices.

Many of schemes proposed for the liquid crystal lenses are based on generating a gradual voltage across the lens capable of reproducing a parabolic refraction index gradient in the LC layer, so mimicking the optical behaviour of a conventional lens.

[*]e-mail: vurruchi@ing.uc3m.es

Voltage gradient can be created by a complex manufacturing process designing a set of electrodes across a thickness-reduced lens and applying zonal control [11]. Patterned electrode method has been reported using dielectric layers between the electrodes and the LC layer causing a parabolic voltage gradient only with optimized distances [12,13]; however, drawback is high control voltages (>50 V_{rms}). Hole patterned method removes the dielectric layers, thus, reducing control voltages but non-optimal relationship between lens aperture and thickness limits the aperture of the lenses [14].

In the last fifteen years, modal control techniques [15] have become an alternative for lens design that lack main drawbacks of the previous techniques. Advantage is the driving method with only one control RMS voltage at low values. First research on modal control was reported by A.F. Naumov *et al*. [16]. This technique consists of generating a radial graded refractive index across aperture lens by using a layer of high resistance sheet (MΩ/sq), deposited onto the pattern electrode as a control electrode. Sheet resistance of the control electrode is a key design parameter. Its value must be in the range of 100 kΩ/sq to few MΩ/sq for lens diameters on the order of millimeters [17]. This layer creates a voltage divider with the LC impedance causing a hyperbolic voltage gradient across the lens aperture [18]. Different materials have been reported to act as a control electrode layer, PEDOT [19], thin ITO layers [20] or titanium oxide films [16]. It is not a simple task, indeed, to obtain the exact thicknesses of the high impedance layer; setting a thickness value must offer a good compromise between impedance (which affects lens refraction index gradient) and transparency (which concerns lens quality). On the other hand, control voltages must be amplitude, frequency and shape-optimized. Due to the capacitive effect of the liquid crystal, LC layer impedance is frequency dependent. In addition, one of the main drawbacks of systems using these optical arrangements is the generation of aberrations. So, the suitable choice of the voltage shape (set of harmonics) can minimize phase aberrations caused by both, non-ideal distribution of the electric field and non-linear electro-optical response of the LC with voltage.

In this work, a special control electrode made by a metallic layer for a tuneable cylindrical lenticular lens array with modal control has been proposed. The main goal is to mimic the behaviour of commercial lenticular lenses employed in lenticular printing which can create different effects on a viewing image such as 3D, animation, flips, morph, zoom, etc. The proposed lenticular devices have the advantage of getting tuneable profiles changing the shape of each lens and also the focal length, thus, allowing the device to provide a 3D effect. LC technology improves lenticular sheet performance for 3D applications because the switching between 2D and 3D modes is achievable without decreasing spatial resolution. Also, an adjustable distance between the observer of the 3D effect and the display can be obtained, unlike conventional lenticular sheet method. The 3D effect can be generated with an auto-stereoscopic system based on a lenticular sheet as depicted in Fig. 1. Stereoscopic vision will result from the appropriate combination of two images received from each eye by the human brain. And the lenticular lens sheet, designed for 3D images, must have a narrow, enough viewing angle (typically, less than 30°).

On the contrary, the so-called flip effect will be created with a wider, enough viewing angle (typically higher than 40°). On both kinds of applications, 3D and flip effect, the pattern on the display will consist of two images specially combined on a display.

2. Lenticular device designing

The key parameter for designing a lenticular lens array is the focal length of each individual lens. In conventional lenses, an approximation of the focal length can be extracted from Fermat's Principle and contributions of Gauss to Gaussian optics [21]. This focal length approximation has been the fundamental theory for designing lenses for many years and is given by

$$f_O = \frac{n_1}{n_2 - n_1} R, \tag{1}$$

where n_1 is the surrounding medium refractive index, n_2 is the refractive index of the lens material and R is the radius of a curvature of the lens. However, new proposal we are con-
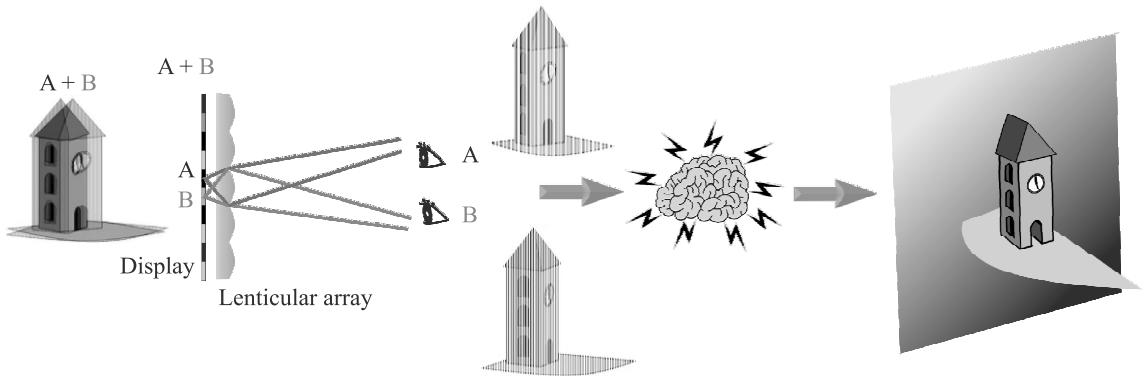

Fig. 1. 3D effect using auto-stereoscopic system based on lenticular lens sheet.

sidering is based on supposing that each lens of the array mimics the effect of a gradient index lens (GRIN). Specifically, for GRIN lenses, the ones where there is a GRadient in the INdex of refraction, an estimation of focal length, f_{GRIN}, becomes simple, taking into account focusing of the parallel rays

$$f_{GRIN} = \frac{R^2}{2d[n_{\max} - n(r)]}, \qquad (2)$$

where R is the lens radius (half lens pitch), d is the thickness of the lens (thickness of the liquid crystal layer) and $n_{max} - n(r)$ is the difference between the maximum refractive index, $n_{\max}$ (at the optical axis of each lens) and the refractive index at the position r (that is at the lens edge). Thus, d can be derived for a particular value of f_{GRIN} according to the application. The specific aim of this work has been focused on designing an optic system based on a lenticular lens array for generating auto-stereoscopic effect inherent in a 3D perception.

In order to avoid adverse effects on vision, an observer should be positioned at the appropriate distance, D, from the screen (Fig. 2). Also, the 3D effect may not be visible when the screen is viewed at an angle. So, designing the focal length of the lenticular array must be defined for a precise position of the observer in front of the device, thus size of the viewing zone is equal or bigger than the interpupillar distance, D_p.

By considering left and right views of the stereogram, so that the observer's eyes see only the respective views of the stereogram, some geometric expressions can be formulated for the angle θ by equations

$$\left.\begin{array}{l} \tan\theta = \dfrac{D_P/2}{D - f} \\[2mm] \tan\theta = \dfrac{P_P/2}{f} \end{array}\right\} \quad f = \frac{DP_P}{D_P + P_P} = 1.093 \text{ mm}. \qquad (3)$$

For the specific prototype manufactured comb control electrodes have been designed as pattern masks for the ITO
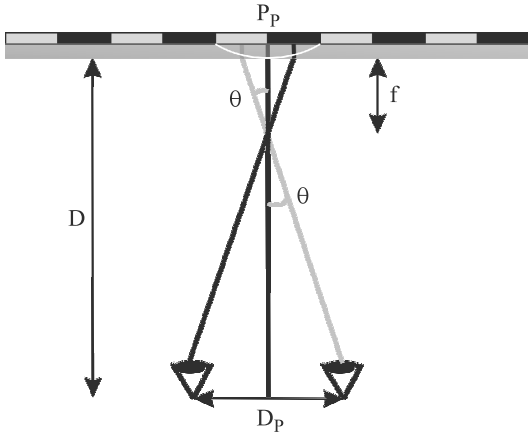

Fig. 2. Scheme of geometry of 3D imaging by lenticular method. D is the distance between observer and lens sheet, P_P is the pixel pitch, and D_P is the interpupillar distance.

on the upper substrate. Distance between teeth of the electrode is the lenticular lens pitch. So, if $D = 50$ cm is the distance between the observer and the lens sheet, $P_p = 142.5$ μm is the pixel pitch and $D_p = 65$ mm is the interpupillar distance, then the focal length becomes $f = 1.093$ mm. This result can be compared with similar results reported in bibliography [22]. The shape of the electrode and the structure of the LC device are shown in Fig. 3.
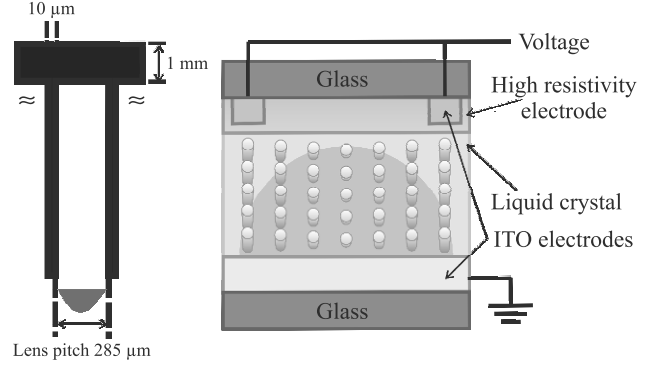

Fig. 3. Structure of LC lenticular lens.

Additionally, the thickness of the device d is a manufacturing parameter of the lenticular device and a design objective. Specifically, for liquid crystal MDA-98-1602 from Merck, with $n_e = 1.7779$ and $n_0 = 1.5113$ (that is $\Delta n = 0.2666$) a focal length about $f_{GRIN} = 1.1$ mm and a lens pitch (double than pixel pitch) of 285 μm, the thickness d becomes

$$d = \frac{R^2}{2\Delta n f_{GRIN}} \Rightarrow d = \frac{(285 \ \mu m/2)^2}{2 \cdot 0.2666 \cdot 1.1 \ mm} = 34.6 \ \mu m. \qquad (4)$$

Thickness value in the final manufactured LC lenticular arrays has been increased by 30%, providing the devices with the additional space to $d = 50$ μm, as in previous results reported in this subject [23]. We have reported bigger focal lengths than expected according to theoretical values, attributing this effect to the saturation in the tilt angle of the molecules as switching, thus, diminishing the effective birefringence inside the device.

Equation (5) allows us, finally, to relate phase shift measurements ($\Delta\Phi$) (considering Fresnel approximation), to focal lengths (f_{GRIN}), in order to confirm the validity of the experimental results for both magnitudes

$$\left.\begin{array}{l} \Delta\Phi = \dfrac{2\pi}{\lambda} \displaystyle\int_{-r}^{r} n_{eff}(\theta)dz = \dfrac{2\pi}{\lambda}\Delta nd \\[3mm] f_{GRIN} = \dfrac{R^2}{2d\Delta n} \end{array}\right\} f_{GRIN} = \frac{\pi R^2}{\lambda\Delta\Phi}. \qquad (5)$$

3. Electro-optical behaviour of lenticular devices

Scope of this work is to compare the performance of LC lenticular lenses with commercial ones. Commercial lenticular sheets with 100 lenses per inch (100 lpi) that is the lens

diameter of 254 μm have been chosen due the similarity between their lens pitches. The comparison has been carried out by two experiments. The first consists of measuring the focal length of both, the LC micro-lenses and the commercial sheets by a simple method. Validity of this measurement scheme will be confirmed by comparing the focal length from this method to the focal length from interference pattern measurements of the devices. The goal of the second experiment is to explore the image generation of basic forms from both lenticular systems.

3.1. Measuring of focal length

In the last years, micro-lenses of many applications are considerably growing in quality and decreasing in prices. However, new approaches and improvements must be necessarily accompanied by characterization systems of the focal length.

First of all, focal length definition for micro-lenses devices must be established. Micro-lens focus is standardized as the distance from the vertex of the micro-lens to the focus position [24]. That position is located by finding the maximum power density distribution as a collimated beam comes into the device surface from the backside. That means that the effective front focal length differs from the classical effective focal length since it is measured from the lens vertex. Also, by reducing the size of the lenses with array structures to a micrometric scale the focal length evaluation is not a simple task by means of mechanical measurements made to a surface of limited aperture lens, such as reciprocal magnification, focal collimation or auto-collimation. So, further research has been directed toward the study of the Gaussian shape of a laser beam [25], the lateral shearing interferometer in transmission [26] or the boundary-element method (BEM) [27]. Particularly in this work, the standardized micro-lens focus definition has been used. Focal length measurements have been tested by the experimental setup shown in Fig. 4. The results are not so critical, due to the LC device plane surface and the accuracy measurement depend on the micro-positioner resolution.

Focusing properties were captured by placing test devices behind a parallel polarizer with the rubbing direction of the lenticular lenses aligned to the main axis of the polarizer. A polarized He-Ne laser beam ($\lambda = 632.8$ nm)

was used as a light source. The high resistivity layer deposited on the control electrode generates an electric field gradient between teeth of the electrode. Consequently, distribution of electric field gives rise to a radial graded refractive index across each lens allowing lens focusing when light passes through the LC device. A micro-positioner has been built to measure the focal length sweeping the position of an X10 objective for finding the focal length. Finally, captured images were recorded by a CCD camera. Figure 5 shows in detail the procedure of measuring the focal length.
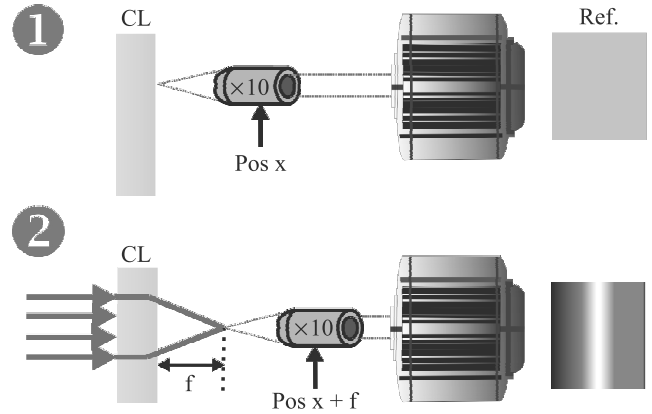

Fig. 5. Detail of procedure for measuring focal lengths.

The procedure involves two steps. The first step consisted of focusing the surface of liquid crystal lens acting as the lens vertex at the initial position x. Next, the micro-positioner is remotely controlled for placing the objective of the distance f from the initial position x capturing the maximum of the power density distribution. The comparison between focusing properties of a cylindrical LC lens array and a commercial lenticular sheet is shown in Fig. 6.

Focal length of a 100 lpi commercial lenticular sheet was 0.74 mm [Fig. 6(a)]. LC lens array focused the laser beam on 1.16 mm [Fig. 6(b)] as a 5.5 V_{rms} square signal was applied to the control electrode. LC lenses and lenticular sheets were both found to be comparable when focusing a collimated laser beam.

On the other hand, viewing angle of both strategies, for getting a 3D effect has been evaluated. This parameter constitutes a typical feature of each lenticular scheme allowing
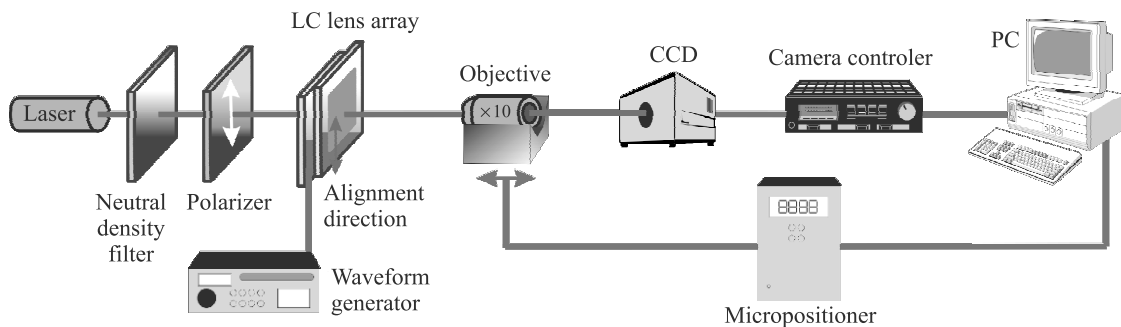

Fig. 4. Experimental set-up for measuring focal lengths of lenticular devices.
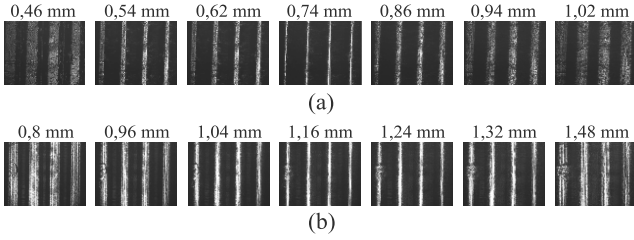
Fig. 6. Comparison between focusing properties of a cylindrical LC lens array and a commercial lenticular sheet: (a) commercial lenticular sheet, (b) cylindrical LC lens array as a 1 kHz-square signal of 5.5 V_{rms} is applied.

us to classify the devices for developing suitable applications intended for them. From Fig. 2 an estimation of the maximum deviation angle of a ray leaving the edge of an individual lens and reaching the corresponding observer's eye, θ_{max}, can be derived as

$$\tan\theta_{max} = \frac{P_P}{f}, \qquad (6)$$

where P_p is the pixel pitch and f is the focal length. By doubling θ_{max} a viewing angle was calculated. After measuring focal lengths, the value of θ_{max} has been obtained from Eq. (6). Viewing angle of the lenticular sheet is 19.5° and 14° for the same of the LC array. Both are values for achievable 3D vision applications with viewing angles typically narrower than 30°. However, the viewing angle of the LC device is narrower than that of the lenticular sheet due to the designing condition of D is fixed at 50 cm. Certainly, that is a consequence derived from the rule: the narrower the viewing angle, the larger the viewing distance for 3D vision.

3.2. Image generation of basic forms

Individual lenses' response of both lenticular sheets and liquid crystal arrays should be comparable at short distances between the observer and the lenticular system. That is, they should generate mirrored images coming from a back display, if the lens pitch size comprises some pixel pitches of the display. For checking that behaviour, the experimental set-up of Fig. 7 was implemented. Some stacks made of two parts, the display and the lenticular system on it, were suitably assembled and placed in the stage of a polarizing microscope. Detail of a stack is depicted on the right side of Fig. 7.

Two basic forms were displayed on the back display [Fig. 8 (a)]. Forms consisted of a set of three consecutive columns of a display (60 μm-pixel pitch), showing a special recognizable pattern. Some captures were recorded by a CCD camera coupled to the microscope, focusing the objective behind the focal lengths of the lenses. Figures 8(b) and 8(c) show the captures for the first stack (lenticular sheet on the display) and the second one (LC lens array onto the display), respectively. The same control voltage than the previous experiment was applied to the LC lens, that is, a 1 kHz-square signal of 5.5 V_{rms}. The result was getting horizontal mirrored images from the original one for both configurations.
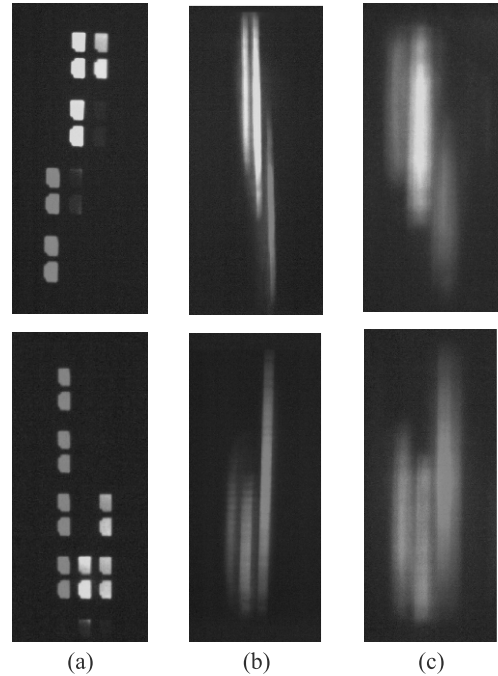

Fig. 8. Captures of inverted images generated from basic forms: (a) two basic forms shown in a RGB display, (b) 100 lpi-lenticular sheet in front of display, and (c) cylindrical LC lens array in front of display.
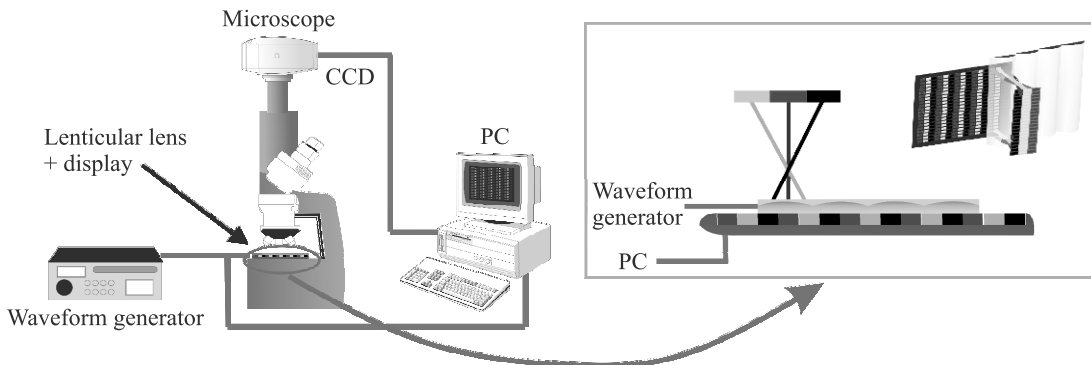

Fig. 7. Experimental set-up for generating inverted images of basic forms.

The main image alterations were spherical and chromatic aberrations produced by the cylindrical LC lens array in image generation. But recently, a mitigation of spherical aberration has been reported in the design of modal lenses [19], as well as aberration corrections with aperture reduction of the lenticular sheet have been proposed for auto-stereoscopic applications [28].

3.3. Phase shift measurements *vs.* focal lengths

Finally, in order to confirm the validity of the experimental focal length measured in the first experimental section, Eq. (5) allows us to obtain the focal length (f_{GRIN}) by the phase shift measurements ($\Delta\Phi$).

So, an experimental set-up based on placing LC lens arrays between two crossed polarizers has been implemented for capturing a typical interference pattern. A polarized He-Ne laser beam ($\lambda = 632.8$ nm) was used as a light source. When linearly polarized light passes through the LC device, ordinary and extraordinary waves experience spatially uniform phase retardation caused by the birefringence of LC, giving rise of a state of polarization change. At this point, the second polarizer blocks 2π phase shifts and let to pass π phase shifts, generating a fringe pattern or interference pattern [Fig. 9(a)].

A×10 objective properly focused was placed in the path of the beam to see correctly the interference pattern handling this task with a micro-positioner. Also, interference fringes were recorded by a CCD camera. To finish, phase profiles [Fig. 9(c)] were obtained from interference patterns [Fig. 9(b)] by a specially developed image recognition program.

The same set-up conditions were established for comparing the results, that is, a 5.5 V_{rms} – and 1 kHz-square signal. The maximum phase shift from the parabolic profile was $\Delta\Phi = 14\cdot2\pi$. By Eq. (5)

$$f_{GRIN} = \frac{\pi R^2}{\lambda\Delta\Phi} = 1.15 \ \text{mm}, \tag{7}$$

where R is half the lens pitch ($285/2$ µm). The focal length designed was at about 1.1 mm, but foreseeing the effects of the non-ideal LC response, cell gap of the manufactured device was increased. The focal length of the LC lens array was at 1.15 mm by the phase method; this result is similar to that previously measured by means of focusing scheme (1.16 mm). The relative error of the focal length has been assessed for both the focusing scheme and the phase method. The absolute error is defined by the difference between the theoretical focal length and the values obtained by some of the previous methods. The relative error is the absolute error divided by the magnitude of the theoretical focal length. For the focusing scheme the relative error is 6.1% and for the phase method it is 5.2%. These results allow us to conclude that both methods are fairly in agreement proving the validity of the two experiments.

4. Conclusions

Comparison between electro-optic behaviour of LC lenticular lenses and commercial lenses, that is lenticular sheets, has been carried out. A specific experimental set-up has been implemented for measuring focal lengths by using a micro-positioner controlled by PC. Focal lengths of a millimetric order have been measured for LC devices. These values have been found to be similar to those of commercial lenticular sheets of a comparable diameter per lens. On a parallel set-up, phase response of LC lenses has been checked. A specific program has been developed to extract the phase profile from the interference pattern. Values of focal lengths obtained from both methods are fairly in agreement. Thus, the use of both methods has been validated. On the other hand, image generation of basic forms has been proved for LC lenses. Horizontal mirrored images have been captured with both kind of devices, LC lenticular lenses and lenticular sheets. In conclusion, the manufactured LC lenses have shown a response comparable to that of commercial lenticular lens arrays. They are promising devices to be used in typical applications of lenticular arrays.

References

1. Gaebler, A. Moessinger, F. Goelden, A. Manabe, M. Goebel, R. Follmann, D. Koether, C. Modes, A. Kipka, M. Deckelmann, T. Rabe, B. Schulz, P. Kuchenbecker, A. Lapanik, S. Mueller, W. Haase, and R. Jakoby, "Liquid crystal-reconfig-
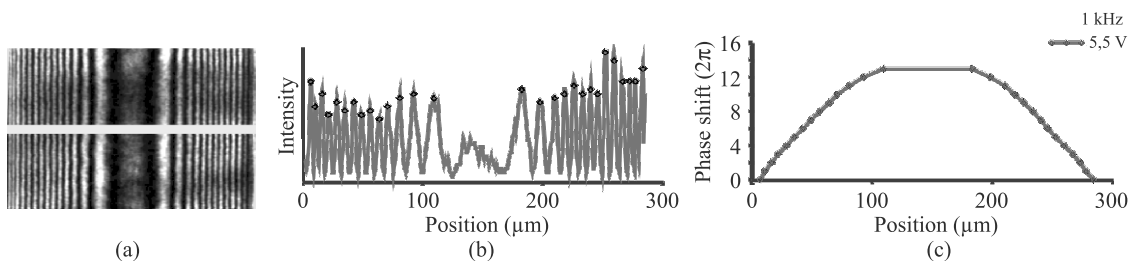
Fig. 9. Phase response of one individual lens of LC lenticular array: (a) Fringe pattern, (b) Intensity profile, (c) Phase profile.

urable antenna concepts for space applications at microwave and millimeter waves", *Int. J. Ant. Prop.* **2009**, 1–7 (2009).

2. X. Wang, T.D. Wilkinson, M. Mann, K.B.K. Teo, and W.I. Milne, "Characterization of a liquid crystal microlens array using multiwalled carbon nanotube electrodes", *Appl. Opt.* **49**, 3311–3315 (2010).

3. Carrasco-Vela, X. Quintana, and E. Otón, "Security devices based on liquid crystals doped with dichroic", *Proc. 7th Spanish Meeting of Optoelectronics*, 2011.

4. W.A. Crossland, T.V. Clapp, T.D. Wilkinson, I.G. Manolis, A. Georgiou, and B. Robertson, "Liquid crystals in telecommunications systems", *Mol. Cryst. Liq. Cryst.* **413**, 2499–2518 (2004).

5. J. Feng, Y. Zhao, S.-S. Li, X.-W. Lin, F. Xu, and Y.-Q. Lu, "Fibre-optic pressure sensor based on tuneable liquid crystal technology", *Photonics Journal IEEE* **2**, 292–298 (2010).

6. E. Otón, D. Poudereux, X. Quintana, J.M. Otón, and M.A. Geday, "Design, manufacturing and characterization of a liquid crystal based blaze grating for space applications", *Proc. 7th Spanish Meeting of Optoelectronics*, 2011.

7. E.J. Fernández, P.M. Prieto, and P. Artal , "Wave-aberration control with a liquid crystal on silicon (LCOS) spatial phase modulator", *Opt. Express* **17**, 11013–11025 (2009).

8. O. Aharon, I. Abdulhalim, O. Arnon, L. Rosenberg, V. Dyomin, and E. Silberstein, "Differential optical spectropolarimetric imaging system assisted by liquid crystal devices for skin imaging", *J. Biomed. Opt.* **16**, 086008-1 − 086008-12 (2011).

9. N. Peyghambarian, G. Li, D. Mathine, and P. Valley, "Electro-optic adaptive lens as a new eyewear", *Mol. Cryst. Liq. Cryst.* **454**, 157–166 (2006).

10. D.W. Berreman, "Variable-focus LC-lens system", US Patent 4 190 330, 1980.

11. G.E. Nevskaya and M.G. Tomilin, "Adaptive lenses based on liquid crystals", *J. Opt. Tech.* **75**, 563–573 (2008).

12. H. Ren, Y. Fan, S. Gauza, and S. Wu, "Tuneable-focus cylindrical liquid crystal lens", *Jpn. J. Appl. Phys.* **43**, 652–653 (2004).

13. M. Ye, B. Wang and S. Sato, "Realization of liquid crystal lens of large aperture and low driving voltages using thin layer of weakly conductive material", *Opt. Express* **16**, 4302–4308 (2008).

14. S. Sato, "Applications of liquid crystals to variable-focusing lenses", *Opt. Rev.* **6,** 471–485 (1999).

15. G.V. Vdovin, I.R. Guralnik, O.A. Zayakin, N.A. Klimov, S.P. Kotova, M.Y. Loktev, and A.F. Naumov, "Modal liquid crystal wave-front correctors", *Bull. Russ. Acad. Sci. Phys.* **72**, 71–77 (2008).

16. A.F. Naumov, M.Y. Loktev, I.R. Guralnik, and G. Vdovin, "Liquid-crystal adaptive lenses with modal control", *Opt. Lett.* **23**, 992–994 (1998).

17. G.D. Love and A.F. Naumov, "Modal liquid crystal lenses", *Liq. Cryst. Today* **10**, 1–4 (2000).

18. S.P. Kotova, V.V. Patlan, and S.A. Samagin, "Tuneable liquid-crystal focusing device. 1. Theory", *Quantum. Electron.* **41**, 58–64 (2011).

19. N. Fraval and J.L.B. de la Tocnaye, "Low aberrations symmetrical adaptive modal liquid crystal lens with short focal lengths", *Appl. Opt.* **49**, 2778–2783 (2010).

20. P.J.W. Hands, A.K. Kirby, and G.D. Love, "Adaptive modally addressed liquid crystal lenses," *Proc. SPIE* **5518**, 136–143 (2004).

21. E. Hecht, *Optics*, Addison Wesley, London, 2002.

22. Y.-Y. Kao, Y.-P. Huang, K.-X. Yang, P.C.-P. Chao, C.-C. Tsai, and C.-N. Mo, "An auto-stereoscopic 3D display using tuneable liquid crystal lens array that mimics effects of GRIN lenticular lens array", *SID International Symposium, Dig. Tech. Pap.* 111–114 (2009).

23. V. Urruchi, J.F. Algorri, J.M. Sánchez-Pena, N. Bennis, M.A. Geday, and J.M. Otón, "Electro-optic characterization of tuneable cylindrical liquid crystal lenses", *Mol. Cryst. Liq. Cryst.* **553**, 211–219 (2012).

24. ISO 14880–1: *Optics and Photonics: Microlens Arrays* Part 1, 2001.

25. A.A. Camacho, C. Solano, M. Cywiak, G. Martínez-Ponce, and R. Baltazar, "Method for the determination of the focal length of a micro-lens" *Opt. Eng.* **39**, 2149–2152 (2000).

26. L. Erdmann and R. Kowarschik, "Testing of refractive silicon micro-lenses by use of a lateral shearing interferometer in transmission", *Appl. Opt.* **37**, 676–682 (1998).

27. J. Liu, B.-Z. Dong, B.-Y. Gu, and G.-Z. Yang, "Entirely electromagnetic analysis of micro-lenses without a beam shaping aperture", *Appl. Opt.* **40**, 1686–1691 (2001).

28. L. Lipton, "Aperture correction for lenticular screens", U.S. Patent no. 7808708B2 (2010).